

Optical properties of $\text{In}_x\text{Ga}_{1-x}\text{N}$ alloys grown by metalorganic chemical vapor deposition

W. Shan,^{a)} W. Walukiewicz, and E. E. Haller

Materials Sciences Division, Lawrence Berkeley National Laboratory, Berkeley, California 94720

B. D. Little and J. J. Song

Center for Laser and Photonics Research and Department of Physics, Oklahoma State University, Stillwater, Oklahoma 74078

M. D. McCluskey and N. M. Johnson

Xerox Palo Alto Research Center, 3333 Coyote Hill Road, Palo Alto, California 94304

Z. C. Feng,^{b)} M. Schurman, and R. A. Stall

EMCORE Corporation, 394 Elizabeth Avenue, Somerst, New Jersey 08873

(Received 18 December 1997; accepted for publication 21 July 1998)

We present the results of optical studies of the properties of $\text{In}_x\text{Ga}_{1-x}\text{N}$ epitaxial layers ($0 < x < 0.2$) grown by metalorganic chemical vapor deposition. The effects of alloying on the fundamental band gap of $\text{In}_x\text{Ga}_{1-x}\text{N}$ were investigated using a variety of spectroscopic techniques. The fundamental band-gap energies of the $\text{In}_x\text{Ga}_{1-x}\text{N}$ alloys were determined using photomodulation spectroscopy measurements and the variation of the fundamental band gap was measured as a function of temperature. The effects of pressure on the band gap for $\text{In}_x\text{Ga}_{1-x}\text{N}$ samples with different alloy concentrations were examined by studying the shift of photoluminescence (PL) emission lines using the diamond-anvil pressure-cell technique. The results show that PL originates from effective-mass conduction-band states. Anomalous temperature dependence of the PL peak shift and linewidth as well as the Stokes shift between photoreflectance and PL lines is explained by composition fluctuations in as-grown InGaN alloys. © 1998 American Institute of Physics. [S0021-8979(98)09520-6]

I. INTRODUCTION

The $\text{In}_x\text{Ga}_{1-x}\text{N}$ alloy system is attracting much attention because of its importance in both scientific and technological aspects. The wavelength of radiation emitted from $\text{In}_x\text{Ga}_{1-x}\text{N}$ can be tuned over a wide range from visible red (~ 610 nm) to ultraviolet (~ 365 nm) by changing the alloy composition and by forming heterostructures such as quantum wells. This property makes $\text{In}_x\text{Ga}_{1-x}\text{N}$ one of the most promising materials for short-wavelength optical applications. As a matter of fact, the importance of $\text{In}_x\text{Ga}_{1-x}\text{N}$ has been demonstrated by the recent breakthroughs that led to the development of optoelectronic devices such as light emitting diodes and laser diodes operating in the blue and ultraviolet spectral regions.¹⁻⁵

The studies performed so far have been focused on the properties of the $\text{In}_x\text{Ga}_{1-x}\text{N}$ alloy system and on device performance and characterization. The vast majority of the investigations have dealt with InGaN/GaN quantum-well (QW) structures.⁶⁻²⁰ Recently, Perlin and coworkers¹⁴ reported that the pressure coefficients of PL and EL emissions from InGaN/GaN/AlGaIn QW samples are much smaller than that of the GaN band gap. The results were explained by assuming that highly localized states, with small pressure coefficients, are involved in the emission processes in the

QWs. Also, anomalous blueshifts in the temperature-dependent luminescence from InGaN QWs based light emitting devices were observed by Eliseev *et al.*¹⁶ and explained by a band-tail-filling model with a Gaussian density of state distribution. The bulk optical properties of $\text{In}_x\text{Ga}_{1-x}\text{N}$ layers were studied in a number of papers^{12,13,16} and several proposals were put forward to explain anomalous features of the light emission processes in this material system. However, there is presently no model that can account for all the characteristics of the luminescence emission from InGaN alloys.

In this article we present the results of a spectroscopic study of the properties of $\text{In}_x\text{Ga}_{1-x}\text{N}$ epitaxial films grown on top of thick GaN epilayers by metalorganic chemical vapor deposition (MOCVD). The advantage of studying alloy epilayers is that it allows us to focus on the optical properties exclusively related to the $\text{In}_x\text{Ga}_{1-x}\text{N}$ alloy system, avoiding the effects of lattice-mismatch induced strain, quantum confinement, and layer thickness fluctuations in InGaN/GaN QW structures. Photoluminescence (PL) measurements were performed to assess the optical properties of samples with different alloy compositions. Photomodulation spectroscopy in both reflection and transmission geometry was used to determine the energy gap of the samples. Further insight into the nature of radiative recombination processes has been attained from measurements of the effects of temperature and pressure on the observed optical transitions in the $\text{In}_x\text{Ga}_{1-x}\text{N}$ samples. By combining several experimental techniques we were able to discriminate between different proposed mechanisms of luminescence emission. We show that the observed

^{a)}Electronic mail: weishan@ux8.lbl.gov

^{b)}Present address: Institute of Materials Research and Engineering, Singapore, 119260.

peculiarities of the optical spectra of InGaN alloys can be consistently explained by large fluctuations of the In composition without any need to invoke highly localized states or strain induced piezoelectric effects.

II. EXPERIMENTAL DETAILS

The InGaN alloy samples used in this work were nominally undoped single-crystal epitaxial films grown by MOCVD. Before the deposition of alloys, thick GaN layers were grown on sapphire substrates at a temperature of ~ 1050 °C with ~ 20 nm GaN buffers. The layers were deposited at a temperature around 800 °C. The thickness of the $\text{In}_x\text{Ga}_{1-x}\text{N}$ epitaxial layers ranges from several hundred to a few thousand Å. The alloy composition of the samples were initially estimated based on the growth conditions and x-ray diffraction (XRD) measurements.^{8,21} However, as reported recently by several groups,^{22–24} InGaN epitaxial layers were found to be pseudomorphically strained to the underlying GaN layers. For this reason, XRD could systematically overestimate InN alloy fraction since it typically measures the *c*-axis lattice constant. Therefore, Rutherford backscattering spectrometry was used to verify In concentrations for the samples.

Optical measurements were carried out on the $\text{In}_x\text{Ga}_{1-x}\text{N}$ samples over a temperature range from 3 K up to room temperature. Samples were mounted onto the cold finger of either a closed-cycle refrigerator or a continuous-flow LHe cryostat and cooled down to the desired temperatures for the measurements. Photoluminescence spectra were recorded using an experimental setup consisting of a HeCd laser as the excitation source and a 1 M double-grating monochromator connected to a photon-counting system. The pressure-dependent PL measurements were carried out on the $\text{In}_x\text{Ga}_{1-x}\text{N}$ alloy samples using gasketed diamond anvil cells (DAC). The pressure medium is a 4:1 methanol/ethanol mixture. In order to accommodate the limited dimensions of the DAC sample space, small sample chips with sizes of $\sim 200 \times 200 \times 30$ μm^3 were prepared by mechanical polishing and cutting. For photomodulation spectroscopy measurements, quasimonochromatic light dispersed by a 1/2 (M) monochromator from a xenon lamp and a chopped HeCd laser modulating beam were focused on the samples and the reflected signals were detected by a UV-enhanced photomultiplier tube connected to a lock-in amplification and data acquisition system.

III. RESULTS

A. Alloying effects

Shown in Fig. 1 are photomodulated transmission (PT) spectra taken at room temperature (295 K) from several $\text{In}_x\text{Ga}_{1-x}\text{N}$ epilayer samples. The derivative-like spectral features marked by vertical arrows in the spectra correspond to the optical transition associated with the band gap of the respective samples. The weaker spectral structure at higher energy seen for the $\text{In}_{0.15}\text{Ga}_{0.85}\text{N}$ sample is caused by the transition from the underlying GaN thick layers. The widths of the PR spectral lines increase with alloy composition. The

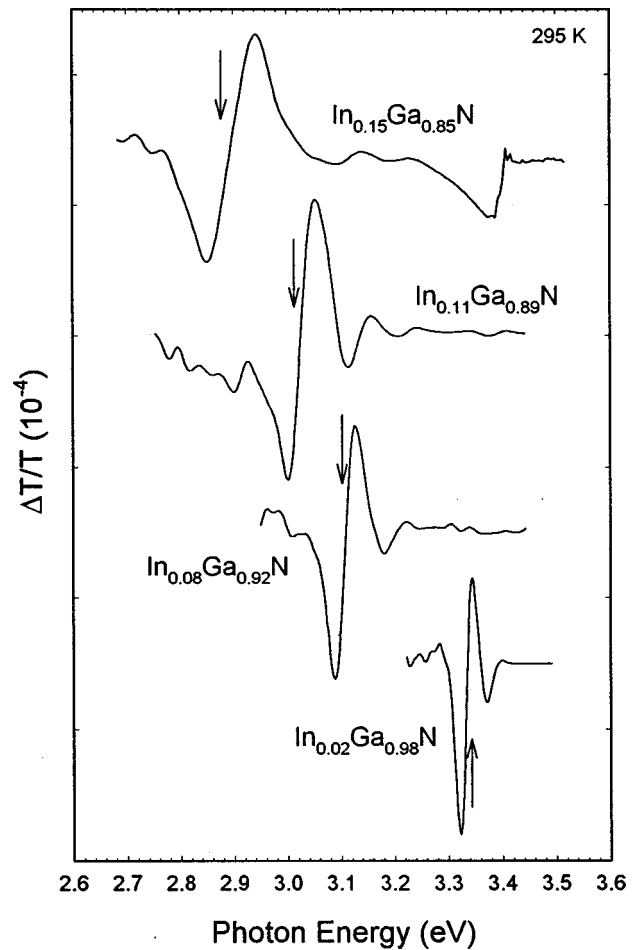


FIG. 1. Photomodulated transmission spectra of $\text{In}_x\text{Ga}_{1-x}\text{N}$ samples taken at room temperature (295 K). The arrows mark the transition energies of the samples.

large difference in transition energies between the samples are clearly due to the change of the fundamental band gap with the composition of InGaN alloys.

The transition energies determined by PT measurements are plotted in Fig. 2 as a function of In concentration. PL peak positions (295 K) of the samples are also presented in the figure. The dashed line in the figure is a least-squares fit to our experimental data using

$$E(x) = E(0) + ax + bx^2, \quad (1)$$

where $E(0)$ is the band gap of GaN at room temperature (~ 3.42 eV),²⁵ x is the InN alloy fraction, and energy is given in eV. The best fit yields $a = -3.91$ and $b = 2.39$ eV with the band gap of InN being fixed at 1.9 eV. McCluskey *et al.*²⁴ reported that the band-gap bowing parameter for the InGaN alloy system is much larger than the value theoretically predicted by first-principles calculations.²⁶ A linear relation between band gap and In concentration for pseudomorphically strained $\text{In}_x\text{Ga}_{1-x}\text{N}$ ($x \leq 0.12$) derived in Ref. 24 (solid line) and the theoretical prediction from Ref. 26 (dotted line) are also shown in Fig. 2 for comparison. A large bowing parameter indicates that alloy disorder has a strong influence on the dependence of energy gaps on the alloy composition, in ad-

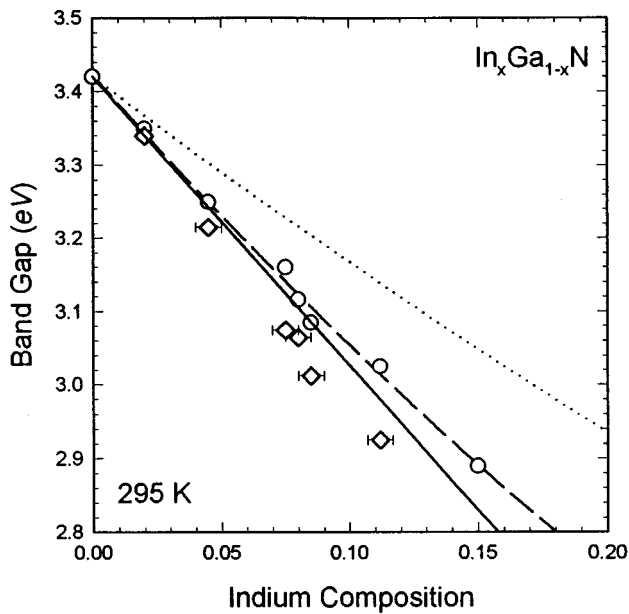


FIG. 2. Transition energy positions for samples with different alloy compositions measured by PT (\circ) and PL (\diamond). The dashed line is the least-squares fit to the experimental PT data. The dotted line is a theoretical prediction for the variation of the band-gap energy for $\text{In}_x\text{Ga}_{1-x}\text{N}$ alloy system (Ref. 26), and the solid line is a linear experimental fit to band gaps of pseudomorphically strained $\text{In}_x\text{Ga}_{1-x}\text{N}$ ($x \leq 0.12$, Ref. 24).

dition to the change of lattice constants. The good agreement between our results and Ref. 24 suggests that the InGaN epilayers studied in this work are pseudomorphically strained to GaN.

B. Temperature dependence

As illustrated in Fig. 2, there exists a Stokes shift between the energy positions determined from PT and PL spectra for all the samples. The magnitude of the shift increases with InN mole fraction. A comparison of a photoreflectance (PR) curve to a PL spectrum taken from an $\text{In}_{0.08}\text{Ga}_{0.92}\text{N}$ sample at room temperature is shown in Fig. 3. The temperature dependence of the energy positions of PL and PR transitions for the sample are shown in Fig. 4. The PR transition energies were determined by fitting PR spectra to a Gaussian line-shape functional form which is appropriate for the optical transitions in an inhomogeneously broadened system.^{27,28} For comparison, the temperature dependence of the peak position of the PL line from the GaN layer in the same sample is also presented in this figure. As expected, the position of the GaN PL line shifts to lower energy with increasing temperature. The total shift of about 60 meV in the temperature range from 10 to 300 K is consistent with previous determinations of the temperature dependence of the GaN energy gap.²⁵ As is seen in Fig. 4, a very similar temperature dependence is found for the optical transition measured by PR in $\text{In}_{0.08}\text{Ga}_{0.92}\text{N}$. In stark contrast, however, we found that the position of the PL line in the same sample is practically independent of temperature in the range from 10 to 200 K. Only a small downward shift of about 20 meV is observed at higher temperatures. In addition, we observed a large Stokes

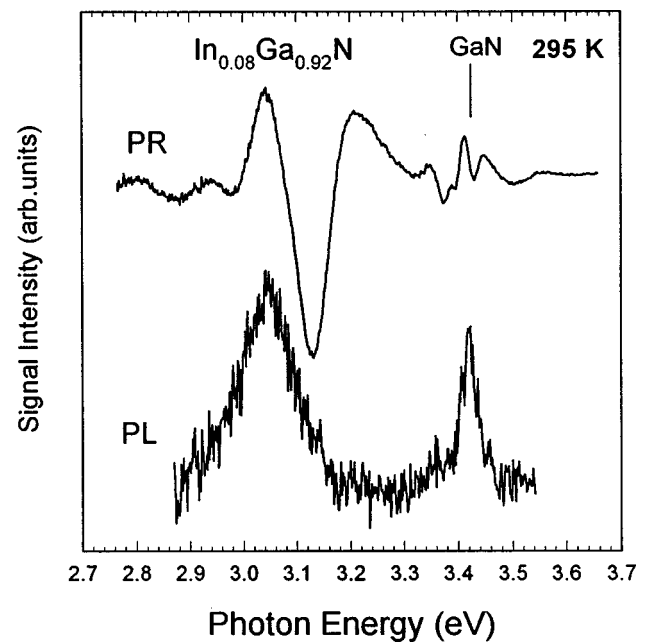


FIG. 3. Comparison of photoreflectance spectrum with PL of an $\text{In}_{0.08}\text{Ga}_{0.92}\text{N}$ sample. Both spectra were taken at room temperature.

shift of about 75 meV between PL and PR peak positions at low temperatures. This shift decreases to about 40 meV at room temperature.

The results presented in Fig. 5 show that there are also significant differences observed in the temperature dependencies of the PL and PR spectral linewidths. The PR spectral feature from the $\text{In}_{0.08}\text{Ga}_{0.92}\text{N}$ sample has a linewidth of about 102 meV at 10 K that slightly increases with temperature to about 120 meV at 300 K. On the other hand, the line shape of the PL spectrum is strongly temperature dependent.

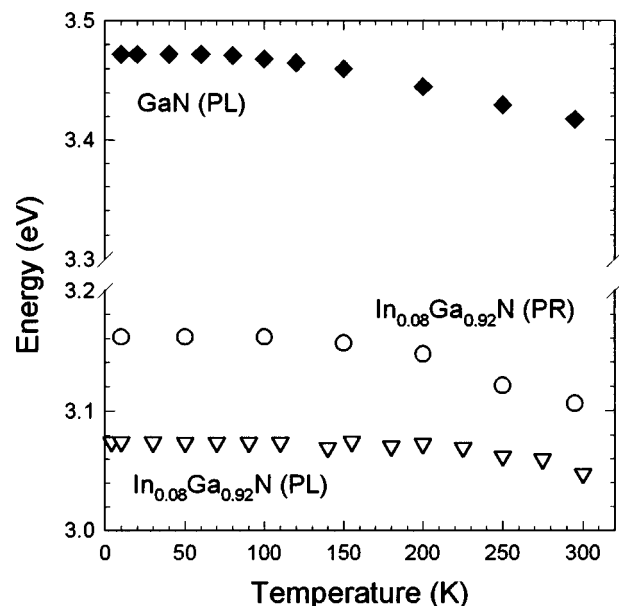


FIG. 4. Variation of transition energies measured by PL and PR for the $\text{In}_{0.08}\text{Ga}_{0.92}\text{N}$ sample, as well as for the underlying GaN layer. Note that the PR transition energy shifts with temperature in the same manner as the GaN excitonic transition.

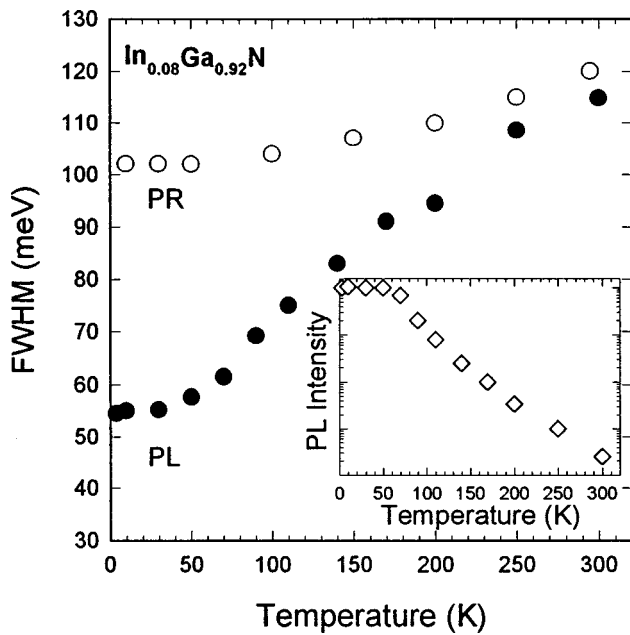


FIG. 5. Effect of temperature on the PL and PR spectral linewidths measured from an $\text{In}_{0.08}\text{Ga}_{0.92}\text{N}$ sample. The inset shows the change of PL intensity as a function of temperature.

A twofold increase of the linewidth is observed in the temperature range from 50 to 300 K. It is important to note that, as is shown in the inset of Fig. 5, the PL intensity is reduced by about three orders of magnitude in the same temperature range.

C. Pressure dependence

The effects of hydrostatic pressure on the PL transitions in GaN and $\text{In}_x\text{Ga}_{1-x}\text{N}$ alloys are shown in Fig. 6. The peak energies of PL emission structures are plotted as functions of pressure. The solid lines in the figure are least-squares fits to the experimental data using the linear-fit function

$$E(P) = E(0) + \alpha P, \tag{2}$$

where the energy E is in eV and the pressure P is in kbar. The yielded pressure coefficients (α) for various samples are listed in Table I.

So far, no experimental results have been reported regarding the pressure coefficient of InN. Theoretical calculations by Christensen and Gorczyca arrived at a pressure coefficient of 3.3×10^{-3} eV/kbar for the band gap of InN.²⁹ These calculations appear to be consistent with our results in that the pressure coefficients of $\text{In}_x\text{Ga}_{1-x}\text{N}$ with small alloy composition do not differ significantly from that of GaN. It should be pointed out that the application of hydrostatic pressure to a sample such as an InGaN epitaxial layer grown on GaN produces an anisotropic strain due to the difference of compressibility between the two materials. The total strain on the InGaN layer under a given amount of pressure is the sum of the strain initially induced by lattice mismatch and the strain induced by applying hydrostatic pressure. Thus the measured pressure coefficients may be slightly affected by contributions from the uniaxial components of the pressure-induced strain tensor.^{30,31} The small variation in the numeri-

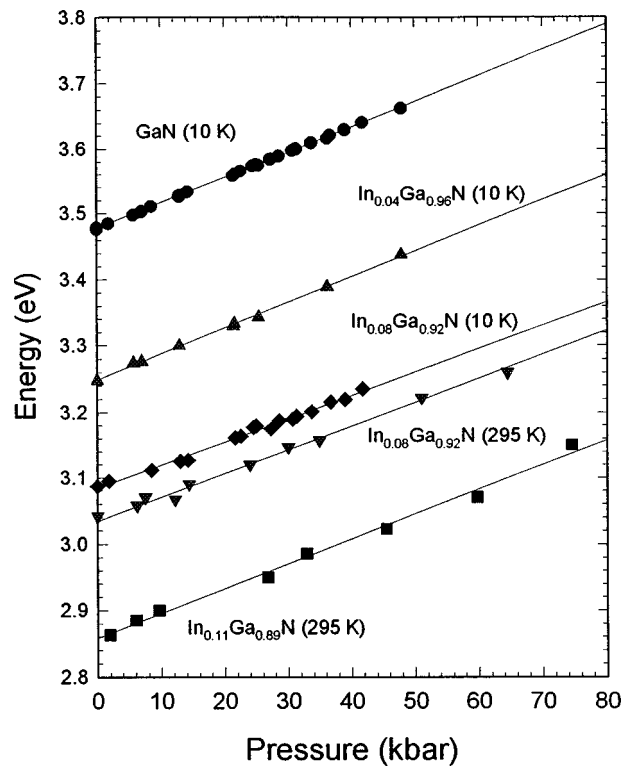


FIG. 6. Shift of PL peak positions with pressure for $\text{In}_x\text{Ga}_{1-x}\text{N}$ samples and the underlying GaN layer.

cal values of pressure coefficients in Table I may arise from this effect. Nevertheless, the most important aspect of the results presented here is that the shift of the luminescence peak position with pressure follows the direct band gap of the $\text{In}_x\text{Ga}_{1-x}\text{N}$ epilayers. This indicates that the electronic states involved in the recombination processes contributing to the PL emissions are associated with the conduction and valence band edges and can be described within the framework of the effective mass approximation. Among such states are the electronic states of the conduction and the valence band extrema and associated excitons as well as shallow donor and acceptor states.

IV. DISCUSSION

One of the most striking features of the optical spectra of InGaN alloys are large linewidths and very large Stokes shifts between PL and PR transition energies. As is shown in Fig. 5 at 10 K, the PL linewidth of about 54 meV is much narrower than the PR linewidth of 102 meV. The PL peak broadens with increasing temperature and approaches the PR

TABLE I. Pressure coefficients of PL emissions in $\text{In}_x\text{Ga}_{1-x}\text{N}$ samples.

	$E(0)$ (eV)	$a = dE/dP$ (10^{-3} eV/kbar)
GaN (10 K)	3.481	3.9
$\text{In}_{0.04}\text{Ga}_{0.96}\text{N}$ (10 K)	3.250	3.9
$\text{In}_{0.08}\text{Ga}_{0.92}\text{N}$ (10 K) ^a	3.085	3.5
$\text{In}_{0.08}\text{Ga}_{0.92}\text{N}$ (295 K) ^a	3.043	3.6
$\text{In}_{0.11}\text{Ga}_{0.89}\text{N}$ (295 K)	2.862	4.0

^aSamples were from two different wafers.

linewidth of 120 meV at room temperature. It is important to note a very distinct correlation between the temperature dependence of the PL linewidth and the PL intensity shown in the inset of Fig. 5. At temperatures below 50 K, both the linewidth and the intensity are almost constant. At higher temperatures the gradually increasing linewidth is accompanied by a dramatic decrease in the intensity. Previous studies have shown that such a decrease in the PL intensity can be attributed to a large reduction of the carrier lifetime.^{7,8}

It has been proposed recently that piezoelectric fields induced by built-in strain are responsible for large PL linewidths observed in InGaN/GaN QW structures and in $\text{In}_x\text{Ga}_{1-x}\text{N}$ epilayers.¹³ To examine the importance of piezoelectric fields in our samples we have measured the dependence of PL spectra on the excitation intensity. It was expected that the screening³² of the internal piezoelectric fields by the photoexcited carriers would result in a blueshift of the PL peak. We have found that changing the excitation intensity by three orders of magnitude does not produce any noticeable shift of the PL line. This result demonstrates that piezoelectric effects do not play any significant role in our samples.

Another interesting characteristic of the InGaN alloys is a very weak temperature dependence of the PL peak position. As is shown in Fig. 4 the PL peak position is practically temperature independent in the temperature range up to 200 K. At higher temperatures the peak shifts to slightly lower energies. This is in contrast to the PR line, which shows typical behavior reflecting the temperature dependence of the energy gap. Also shown in Fig. 4 is the temperature dependence of the PL line in GaN. Again in this case we find that the peak follows the temperature dependence of the energy gap.

A similar weak dependence of the PL peak position on temperature in InGaN alloys was reported by Chichibu *et al.*¹² They assigned the observed luminescence emission to bound, localized states in their InGaN samples. It is well known that localized states have pressure dependence smaller, in most instances, than the band edge states. However, our pressure-dependent PL results shown in Fig. 6 indicate that the pressure coefficient of the PL line is the same as that of the conduction-band edge. This is strongly suggestive that the near-band-edge PL signal results from radiative decay between effective-mass states and that no highly localized states are involved in the process.

All the above results indicate that the alloying of InN with GaN produces drastic changes in the material optical characteristics. The effects of alloying on the PL linewidth were previously extensively studied in other III-V semiconductors. The broadening of the emission lines in AlGaAs semiconductor alloys was attributed to the random fluctuations of the alloy composition.^{33,34} Assuming a completely disordered alloy and neglecting any charge localization effects one obtains the following expression for the emission linewidth:³³⁻³⁵

$$I(E) = (2\pi)^{-1/2} (1/\sigma) \exp\left\{-\left[\frac{E - E_0}{2\sigma}\right]^2\right\}, \quad (3)$$

where E_0 is the transition energy and σ is the standard deviation of band-gap energy given by

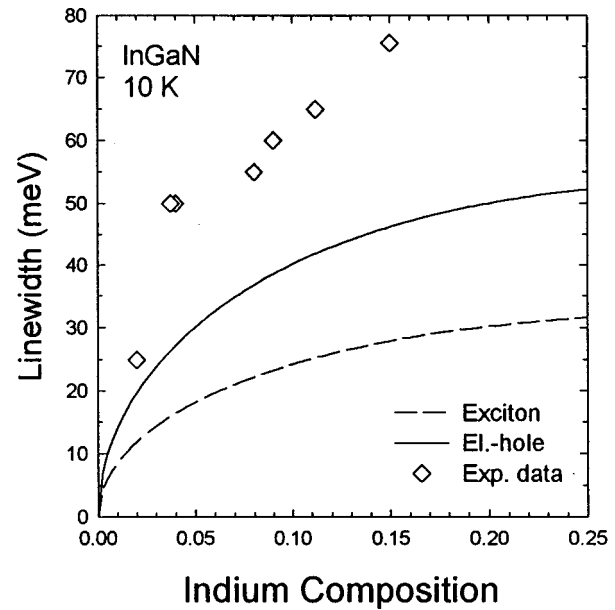


FIG. 7. Comparison of measured and calculated PL linewidths. The calculated linewidth takes into account the statistical alloy fluctuations only. The electron-hole and the excitonic transitions are represented by the solid and the broken lines, respectively.

$$\sigma = [3a_0^3x(1-x)/16\pi r^3] dE_g/dx, \quad (4)$$

where dE_g/dx is the change of the band-gap energy with alloy composition, a_0 is the lattice constant, and r is the Bohr radius for the charge carriers (electron and hole) or excitons, depending on the nature of recombination. The PL linewidths calculated from Eqs. (3) and (4) is shown in Fig. 7. It is clear that the observed PL linewidths are much larger than those calculated assuming a statistically random distribution of In. In fact, more recent work has shown that Eq. (4) overestimates the linewidth by a factor of ~ 2.45 ,³⁶ making the disagreement between theory and experiment even more obvious. This supports the inference that the shape of the emission line cannot be explained by statistically random alloy disorder.

One might wonder whether the effects of compressive strain, as in the case of InGaN pseudomorphically strained to GaN, may broaden the lineshape of an optical transition since the strain induces, in addition to a net increase of band-gap energy, further splitting of the top of the valence bands. If the broadening of the PR and PL spectral features are predominantly due to this splitting, the temperature dependence of PR and PL transition energies should be expected to be very similar to each other. However, the observed anomalous temperature-dependent PL peak shift rules out the significance of strain on the PR and PL linewidth broadening.

Several recent studies have suggested that a strong immiscibility of InN in a nitride ternary alloy leads to a phase separation resulting in compositional inhomogeneities much larger than would be expected from statistical randomness.^{19,20} Here we show that the existence of such inhomogeneities can provide a basis for a qualitative explanation of the optical spectra in InGaN alloys. Positions of the conduction and valence band edges in InGaN with spatial

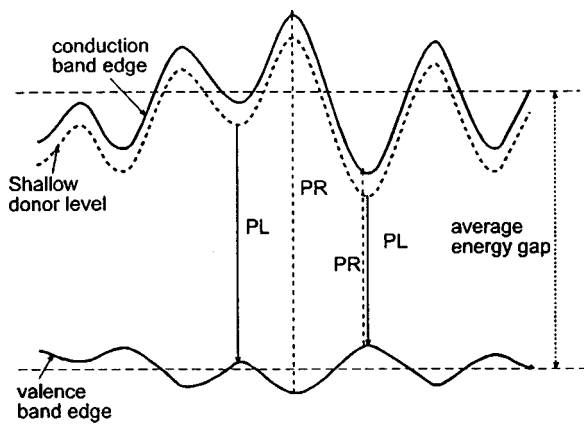


FIG. 8. Schematic representation of PL and PR transitions in inhomogeneous InGaN alloys. The solid vertical lines qualitatively indicate the lower and upper limits of the energy range involved in the PL transition. The vertical broken lines mark the limits of the energy range which contribute to the PR signal.

variations of the alloy composition are schematically shown in Fig. 8. Because of the large ratio of the conduction to the valence band offsets ($\Delta E_c/\Delta E_v=5$),³⁷ most of the change in the band gap is accommodated by the variation in the conduction-band edge energy. Also, since as-grown InGaN is always *n* type, we expect a significant density of states below the conduction-band edge. The effective-mass shallow donor states are delocalized and therefore they closely follow the conduction band edge.

The optical transitions contributing to the PR spectrum involve both the valence and conduction-band edge states. The contribution from the transitions between the valence band and the shallow donor states is much smaller than the band-to-band contribution and therefore can be safely ignored. Assuming a Gaussian distribution for the band edge energies:

$$D(E) = (2\pi)^{-1/2} \int D(E-E')(1/\sigma) \times \exp\{-[(E-E_0)/2\sigma]^2\} dE', \quad (5)$$

the value of σ can be obtained from $W_{PR}=2.35\sigma$, the linewidth of the PR spectrum. This leads to $\sigma=43$ meV for the results shown in Fig. 5 with the low temperature $W_{PR}=102$ meV. Using Eq. (1) that relates the energy gap to the alloy composition in InGaN we found that the standard deviation of $\sigma=43$ meV in the band gap corresponds to about 2.9% standard deviation in the alloy composition.

Within this picture we can also qualitatively understand the origin of the large Stokes shift of the PL line. In the PL process, photoexcited electrons relax by diffusing to the lowest available energy state. Then they recombine with holes in the valence band. As is shown in Fig. 8, we assume that the low energy states are shallow impurity states associated with local minima in the conduction band. By definition the local minima are mostly located below the average conduction-band edge that corresponds to the transition energy for the PR spectral feature. Therefore one expects that the PL linewidth will be approximately equal to half of the PR line-

width. This rough estimate is in a good agreement with the experimental results shown in Fig. 5, where $W_{PR}=102$ meV and $W_{PL}=54$ meV were found.

The position of the maximum PL peak is approximately given by

$$E_{PL} = E_{PR} - W_{PL}/2 - E_d, \quad (6)$$

where E_{PR} is the energy position of the band-to-band transition determined by PR and E_d is the shallow donor binding energy. Adopting a value of 30 meV for the binding energy E_d (effective-mass hydrogenic model) we obtain 57 meV for the Stokes shift between PR and PL lines. Considering the very crude nature of our estimates, this value is in reasonably good agreement with the experimentally observed low-temperature shift of about 75 meV.

So far we have assumed that the nonradiative lifetime is long enough for electrons to diffuse to the local minima before recombining with holes. This is true at low temperatures when PL lifetimes in excess of a few hundred picoseconds (ps) are typically observed in these materials.^{7,8} However, it has been reported that the PL lifetime decreases very rapidly with increasing temperature. Lifetimes of less than 20 ps were measured at room temperature.⁸ This behavior is indirectly evident in our samples where, as shown in Fig. 5, a very rapid reduction of the PL intensity is observed for temperatures higher than 50 K. Shortening of the nonradiative lifetime changes the kinetics of the PL process. The diffusion length of photoexcited carriers is reduced and they are not able to diffuse to a local minimum. Thus more and more electrons with energies exceeding the average conduction-band edge contribute to the PL signal. This obviously leads to a broadening and a shift to higher energy of the PL spectrum. In the limit of very short lifetime the PL linewidth should approach that of the PR spectrum. The results in Fig. 5 show that this is exactly what is observed in our samples.

It is now quite easy to understand the differences in the temperature dependence of the PR and PL energy positions shown in Fig. 4. The PR energy position is defined by the average energy gap that has a very similar temperature dependence to an energy gap in a homogenous material such as GaN. On the other hand, as we have argued above, the PL peak position shifts to higher energy with increasing temperature. At temperatures below 200 K this shift compensates for a downward shift of the band gap resulting in a temperature independence of the PL peak position. A small downward shift of the PL peak position is observed at $T > 200$ K when the change in the band gap is more strongly dependent on temperature.

V. CONCLUSIONS

Pressure and temperature dependencies of the optical properties of $\text{In}_x\text{Ga}_{1-x}\text{N}$ alloys have been studied using photoluminescence measurements and photomodulation spectroscopy. Highly sensitive photomodulation spectroscopy allowed us to determine the average band-gap energy as a function of In content. The pressure-dependent PL measurements indicate that the low-energy states contributing to the low temperature PL signal follow the band edges and there-

fore can be treated within the effective mass approximation. The pressure coefficients of the direct band gaps of several $\text{In}_x\text{Ga}_{1-x}\text{N}$ samples with $0 < x < 0.2$ were deduced from the pressure dependencies of the radiative decay of the charge carriers localized in those tail states. The anomalous temperature dependence of the PL peak shifts and the linewidth have been qualitatively explained in terms of spatial fluctuations of In content. The fluctuations are much larger than predicted for completely random alloys indicating a phase separation in as grown InGaN alloys.

ACKNOWLEDGMENTS

The authors are pleased to thank K. M. Yu for the RBS measurements and gratefully acknowledge the helpful discussions with P. Perlin. This work was performed under a Cooperative Research and Development Agreement (CRADA) with Hewlett Packard Laboratories and was supported by the Director, Office of Energy Research, Office of Computational and Technology Research, of the U.S. Department of Energy under Contract No. DE-AC03-76SF00098. The work at OSU was supported by AFOSR, ARO, DARPA, and ONR.

- ¹S. Nakamura, *J. Vac. Sci. Technol. A* **13**, 705 (1995), and references therein.
- ²S. Nakamura, M. Senoh, S. Nagahama, N. Iwasa, T. Yamada, T. Matsushita, H. Kiyoku, and Y. Sugimoto, *Jpn. J. Appl. Phys., Part 2* **35**, L74 (1996).
- ³I. Akasaki, S. Sota, H. Sakai, T. Tanaka, M. Koike, and H. Amano, *Electron. Lett.* **32**, 1105 (1996).
- ⁴K. Itaya, M. Onomura, J. Nishio, L. Sugiura, S. Saito, M. Suzuki, J. Rennie, S. Y. Nunoue, M. Yamamoto, H. Fujimoto, Y. Kokubun, Y. Ohba, G. I. Hatakoshi, and M. Ishikawa, *Jpn. J. Appl. Phys., Part 2* **35**, L1315 (1996).
- ⁵S. Nakamura, M. Senoh, S. Nagahama, N. Iwasa, T. Yamada, T. Matsushita, Y. Sugimoto, and H. Kiyoku, *Appl. Phys. Lett.* **70**, 1417 (1997).
- ⁶S. Keller, B. P. Keller, D. Kapolnek, A. C. Abare, H. Masui, L. A. Coldren, U. K. Mishra, and S. P. DenBaars, *Appl. Phys. Lett.* **68**, 3147 (1996).
- ⁷M. Smith, G. D. Chen, J. Y. Lin, H. X. Jiang, M. Asif Khan, and Q. Chen, *Appl. Phys. Lett.* **69**, 2837 (1996).
- ⁸W. Shan, B. D. Little, J. J. Song, Z. C. Feng, M. Schurman, and R. A. Stall, *Appl. Phys. Lett.* **69**, 3315 (1996).
- ⁹S. Chichibu, T. Azuhata, T. Sota, and S. Nakamura, *Appl. Phys. Lett.* **69**, 4188 (1997).
- ¹⁰E. S. Jeon, V. Kozlov, Y. K. Song, A. Verkikov, M. Kuball, A. V. Nurmikko, H. Liu, C. Chen, R. S. Kern, C. P. Kuo, and M. G. Craford, *Appl. Phys. Lett.* **69**, 4194 (1996).
- ¹¹Y. Narakawa, Y. Kamakami, M. Funato, Sz. FujiTa, Sg. Fujita, and S. Nakamura, *Appl. Phys. Lett.* **70**, 981 (1997); *Phys. Rev. B* **55**, R1938 (1997).
- ¹²S. Chichibu, T. Azuhata, T. Sota, and S. Nakamura, *Appl. Phys. Lett.* **70**, 2822 (1997).
- ¹³K. P. O'Donnell, T. Breitkopf, H. Kalt, W. Van der Stricht, I. Moerman, P. Demeester, and P. G. Middleton, *Appl. Phys. Lett.* **70**, 1843 (1997).
- ¹⁴P. Perlin, V. Iota, B. A. Weinstein, P. Wisniewski, T. Suski, P. G. Eliseev, and M. Osinski, *Appl. Phys. Lett.* **70**, 2993 (1997).
- ¹⁵C.-K. Sun, T.-L. Chiu, S. Keller, G. Wang, M. S. Minsky, S. P. DenBaars, and J. E. Bowers, *Appl. Phys. Lett.* **71**, 425 (1997).
- ¹⁶P. G. Eliseev, P. Perlin, J. Y. Lee, and M. Osinski, *Appl. Phys. Lett.* **71**, 569 (1997).
- ¹⁷A. Wakahara, T. Tokuda, X. Z. Dang, S. Noda, and A. Sasaki, *Appl. Phys. Lett.* **71**, 906 (1997).
- ¹⁸P. A. Grudowski, C. J. Eiting, J. Park, B. S. Shelton, D. J. H. Lambert, and R. D. Dupuis, *Appl. Phys. Lett.* **71**, 1537 (1997).
- ¹⁹S. Chichibu, K. Wada, and S. Nakamura, *Appl. Phys. Lett.* **71**, 2346 (1997).
- ²⁰M. D. McCluskey, L. T. Romano, B. S. Krusor, D. P. Bour, N. M. Johnson, and S. Brennan, *Appl. Phys. Lett.* **72**, 1730 (1998).
- ²¹W. Shan, J. J. Song, Z. C. Feng, M. Schurman, and R. A. Shall, *Appl. Phys. Lett.* **71**, 2433 (1997).
- ²²T. Takeuchi, H. Takeuchi, S. Sota, H. Sakai, H. Amano, and I. Akasaki, *Jpn. J. Appl. Phys., Part 2* **36**, L177 (1997).
- ²³L. T. Romano, B. S. Krusor, M. D. McCluskey, D. P. Bour, and K. Nuaka, *Appl. Phys. Lett.* (to be published).
- ²⁴M. D. McCluskey, C. G. Van de Walle, C. P. Master, L. T. Romano, and N. M. Johnson, *Appl. Phys. Lett.* **72**, 2725 (1998).
- ²⁵W. Shan, T. Schmidt, X. H. Yang, S. J. Hwang, J. J. Song, and B. Goldenberg, *Appl. Phys. Lett.* **66**, 985 (1995).
- ²⁶A. F. Wright and J. S. Nelson, *Appl. Phys. Lett.* **66**, 3051 (1995).
- ²⁷F. H. Pollak and O. J. Glembocki, *Proc. SPIE* **946**, 2 (1988).
- ²⁸O. J. Glembocki and B. V. Shanabrook, *Superlattices Microstruct.* **5**, 235 (1987).
- ²⁹N. E. Christensen and I. Gorczyca, *Phys. Rev. B* **50**, 4397 (1994).
- ³⁰B. Rockwell, H. R. Chandrasekhar, M. Chandrasekhar, A. K. Ramadas, M. Kobayashi, and R. L. Gunshor, *Phys. Rev. B* **44**, 11307 (1991).
- ³¹J. A. Tuchman and I. P. Herman, *Phys. Rev. B* **45**, 11929 (1991).
- ³²See, for example, B. K. Ridley, *Quantum Process in Semiconductors* (Clarendon, Oxford, 1982).
- ³³E. F. Schubert, E. O. Göbel, Y. Horikoshi, K. Ploog, and H. J. Queisser, *Phys. Rev. B* **30**, 813 (1984).
- ³⁴E. F. Schubert and K. Ploog, *J. Phys. C* **18**, 4549 (1985).
- ³⁵E. F. Schubert and W. T. Tsang, *Phys. Rev. B* **34**, 2991 (1986).
- ³⁶J. M. Langer, R. Buczko, and A. M. Stoneham, *Semicond. Sci. Technol.* **7**, 547 (1992).
- ³⁷C. G. Van de Walle and J. Neugebauer, *Appl. Phys. Lett.* **70**, 2577 (1997).